Identification of the Metal-Binding Sites of Restriction Endonucleases by Fe^{2+}-Mediated Oxidative Cleavage

John J. Hlavaty, Jack S. Benner, Linda J. Hornstra, and Ira Schildkraut*

New England Biolabs, 32 Tozer Road, Beverly, Massachusetts 01915

Received September 29, 1999; Revised Manuscript Received January 10, 2000

ABSTRACT: Fenton chemistry [Fenton (1894) *J. Chem. Soc*. *65*, 899−910] techniques were employed to identify the residues involved in metal binding located at the active sites of restriction endonucleases. This process uses transition metals to catalytically oxidize the peptide linkage that is in close proximity to the amino acid residues involved in metal ligation. Fe^{2+} was used as the redox-active transition metal. It was expected that Fe^{2+} would bind to the endonucleases at the Mg^{2+}-binding site [Liaw et al. (1993) *Biochemistry 32*, 7999−4003; Ermácora et al. (1992) *Proc. Natl. Acad. Sci. U.S.A. 89*, 6383−6387; Soundar and Colman (1993) *J. Biol. Chem. 268*, 5264−5271; Wei et al. (1994) *Biochemistry 33*, 7931−7936; Ettner et al. (1995) *Biochemistry 34*, 22−31; Hlavaty and Nowak (1997) *Biochemistry 36*, 15515−15525). Fe^{2+}-mediated oxidation was successfully performed on *Taq*I endonulease, suggesting that this approach could be applied to a wide array of endonucleases [Cao and Barany (1998) *J. Biol. Chem. 273*, 33002−33010]. The restriction endonucleases *Bam*HI, *Fok*I, *Bgl*I, *Bgl*II, *Pvu*II, *Sfi*I, *Bss*SI, *Bso*BI, *Eco*RI, *Eco*RV, *Msp*I, and *Hin*P1I were subjected to oxidizing conditions in the presence of Fe^{2+} and ascorbate. All proteins were inactivated upon treatment with Fe^{2+} and ascorbate. *Bam*HI, *Fok*I, *Bgl*I, *Bgl*II, *Pvu*II, *Sfi*I, *Bss*SI, and *Bso*BI were specifically cleaved upon treatment with Fe^{2+}/ascorbate. The site of Fe^{2+}/ascorbate-induced protein cleavage for each enzyme was determined. The Fe^{2+}-mediated oxidative cleavage of *Bam*HI occurs between residues Glu77 and Lys78. Glu77 has been shown by structural and mutational studies to be involved in both metal ligation and catalysis [Newman et al. (1995) *Science 269*, 656−663; Viadiu and Aggarwal (1998) *Nat. Struct. Biol. 5*, 910−916; Xu and Schildkraut (1991) *J. Biol. Chem. 266*, 4425−4429]. The sites of Fe^{2+}/ascorbate-induced cleavage for *Pvu*II, *Fok*I, *Bgl*I, and *Bso*BI agree with the metal-binding sites identified in their corresponding three-dimensional structures or from mutational studies [Cheng et al. (1994) *EMBO J. 13*, 3297−3935; Wah et al. (1997) *Nature 388*, 97−100; Newman et al. (1998) *EMBO J. 17*, 5466−5476; Ruan et al. (1997) *Gene 188*, 35−39]. The metal-binding residues of *Bgl*II, *Sfi*I, and *Bss*SI are proposed based on amino acid sequencing of their Fe^{2+}/ascorbate-generated cleavage fragments. These results suggest that Fenton chemistry may be a useful methodology in identifying amino acids involved in metal binding in endonucleases.

The active sites of seven restriction endonucleases, *Bam*HI, *Fok*I, *Cfr*10I, *Eco*RI, *Eco*RV, *Bgl*I, and *Pvu*II, whose three-dimensional structures have been determined (*1*−*8*), are structurally similar to each other. The critical catalytic amino acids of *Bam*HI, Glu77, Asp94, and Glu111 have corresponding residues found in *Eco*RI (Asp59, Asp91, and Glu111), *Eco*RV (Glu45, Asp74, and Asp90), *Bgl*I (Glu87, Asp116, and Asp142), and *Pvu*II (Glu55, Asp58, and Glu68). *Bam*HI has the additional critical carboxylic acid residue at Glu113 where this position corresponds to a lysine residue for *Eco*RI (Lys113), *Eco*RV (Lys92), *Bgl*I (Lys144), and *Pvu*II (Lys70). For each enzyme, it has been proposed that the first three critical amino acids are involved in metal binding. Despite the occurrence of similar amino acids at the active sites of these enzymes, there is no significant sequence homology among Type II restriction endonucleases. It is difficult to align the sequences of endonucleases based solely on the above four active site amino acid residues. Knowing the amino acid sequence of a restriction endonuclease is generally not sufficient to identify which amino acids are critical for catalysis.

In an attempt to identify the amino acids involved in metal binding at the active sites of endonucleases, Fenton chemistry techniques (*9*) were explored. This process uses transition metals to catalytically oxidize chelating ligands with deleterious effects. In the past, Fenton chemistry methods have been employed to explore the reactions of ligand−DNA complexes. More recently, Schepartz and Cuenoud (*10*) and Hoyer et al. (*11*) applied Fenton chemistry techniques to investigate the active sites of proteins by using reagents which specifically and oxidatively cleave the polypeptide backbones of enzymes at their metal-binding sites. Often, a redox-capable metal ion that has a particular affinity for the enzyme is employed in the reaction. A number of studies indicate that Fe^{2+} causes oxidative cleavage of proteins (*12*−*19*). The metal-catalyzed oxidation generates reactive species ($O^{\bullet -}_2$ or OH) through Fenton chemistry (*9*). The reactive species can interact with nearby susceptible amino acid residues and can specifically cleave the polypeptide backbone in close proximity to the site where reactive species are generated.

* To whom correspondence should be addressed. Phone: (978) 927-5054. Fax: (978) 921-1350. E-mail: schildkr@neb.com.

10.1021/bi992268c CCC: $19.00
Published on Web 02/24/2000

Farber and Levine (*12*) and, later, Liaw et al. (*13*) demonstrated that the metal ligands of glutamine synthetase could be identified by treating the enzyme with Fe^{2+} and ascorbate. Glutamine synthetase was inactivated and specifically cleaved upon incubation with Fe^{2+} and ascorbate. The resulting peptides were separated and sequenced to identify the metal-binding site. Similar work was performed on the proteins staphylococcal nuclease (*14*), isocitrate dehydrogenase (*15*), malic enzyme (*16*), Tet Repressor (*17*), phosphoenolpyruvate carboxykinase (*18*), and, recently, *Taq*I endonuclease (*19*). In each case, the modification is selective for the metal binding site of the protein.

Here, Fenton chemistry techniques were applied to the restriction endonucleases, *Bam*HI *Pvu*II, *Fok*I, *Bgl*I, *Eco*RI, and *Eco*RV, whose three-dimensional structures have been resolved (*1*−*3*, *5*−*8*), as well as *Bgl*II, *Sfi*I, *Bss*SI, *Bso*BI, *Hin*P1I, and *Msp*I. The effects of Fe^{2+}/ascorbate-induced endonuclease inactivation and cleavage were characterized in the greatest detail with *Bam*HI. While all 12 enzymes were inactivated following treatment with Fe^{2+}/ascorbate, only eight endonucleases, *Bam*HI, *Pvu*II, *Fok*I, *Bgl*I, *Bgl*II, *Sfi*I, *Bso*BI, and *Bss*SI, were specifically cleaved, suggesting that under appropriate conditions some endonucleases are susceptible to oxidative cleavage at distinct sites. Sequencing of the cleavage products for *Bam*HI, *Pvu*II, *Fok*I, *Bgl*I, and *Bso*BI indicated that the enzymes were oxidatively cleaved at their respective metal-binding sites as identified by their corresponding three-dimensional structures or mutational studies (*1*−*3*, *7*, *8*, *20*). These results suggest that Fenton chemistry techniques can be utilized on a variety of endonucleases in order to gain more information about the catalytic sites of these enzymes.

MATERIALS AND METHODS

Materials. Chelex-100 was from Bio-Rad. Ascorbic acid was from Fisher. All other reagents were of the highest purity commercially available. All nonmetal solutions were passed through a Chelex-100 column to remove any contaminating metal ions. Metal solutions were prepared with ddH_2O which was passed through a Chelex-100 column and adjusted to pH 4.0. All restriction enzymes, DNA substrates, and protein and DNA molecular mass markers were from New England Biolabs. The Asp58Ala mutant of *Pvu*II was a kind gift from Paul Riggs at New England Biolabs.

For all work presented here, each enzyme was dialyzed against 10 mM Tris-HCl[1] (pH 7.9) with 100 mM KCl. Each enzyme was then treated with Chelex-100 prior to use by adding the dialyzed enzyme (approximately 100 μL) to an Eppendorf tube containing approximately 25 μL of Chelex-100 resin. The tube was gently shaken and quick-spun using a minicentrifuge to pellet the resin. The supernatant, which contained the enzyme, was removed. All enzyme concentrations were determined with the Bio-Rad Protein Assay System using BSA as a standard.

pUC19 DNA was linearized with *Bsr*FI endonuclease prior to use in activity measurements of *Bam*HI. Linearized pUC19 DNA was extracted with phenol/chloroform and chloroform and precipitated with ethanol. The DNA pellet was washed with 70% ethanol and resuspended in 0.5 mM EDTA and 10 mM Bis-Tris-Propane (pH 7.4).

BamHI Assay. The nuclease activity of *Bam*HI was determined by titrating the endonuclease in a reaction mix (20 μL total) containing 0.2 μg of *Bsr*FI linearized pUC19 DNA, 100 mM KCl, 10 mM $MgCl_2$, 1 mM DTT, 1 mM EDTA, 10 mM Bis-Tris-Propane (pH 7.4), and 0.2 μg of BSA. After 30 min at 25 °C, the reaction was terminated by the addition of a stop dye solution [4 μL of 0.15% (w/v) bromophenol blue, 25% glycerol, 100 mM Tris-HCl (pH 8), 100 mM EDTA (pH 8) and 5% (w/v) SDS]. The DNA fragments were separated by gel electrophoreses (1% agarose gel in TBE buffer containing 0.01% ethidium bromide). The UV-illuminated gel images were digitally photographed and the DNA bands were quantified using the computer program NIH Image software (version 1.59). The nuclease activity of all other enzymes was monitored using λ DNA under the appropriate assay conditions (*22*).

Fe^{2+}/Ascorbate Treatment. Ferrous sulfate (20−1000 μM) was added to 2 μM endonuclease in 50 mM Tris-HCl buffer, pH 7.4. The solution was incubated for 15 min on ice followed by the addition of ascorbate (1−10 mM). The solution then sat on ice or at room temperature for an additional period of 30 min to 24 h. Enzyme solutions were then tested for nuclease activity and for protein cleavage.

*Bam*HI inactivation was monitored by removing an enzyme aliquot at selected time intervals, quenching the reaction by the addition of 10 mM EDTA and assaying for enzymatic activity by addition to a *Bam*HI reaction assay mix 50-fold larger by volume. *Bam*HI inactivation rate constants were calculated as first-order constants from the slope of the line as determined from the plots of log % activity vs time.

Protection against Fe^{2+}/Ascorbate-Induced Inactivation and Cleavage. Protection against Fe^{2+}/ascorbate-induced *Bam*HI inactivation and/or cleavage was determined by incubating the enzyme with 4 mM of $MgCl_2$, $CoCl_2$, $MnCl_2$, $CuCl_2$, or $CaCl_2$ prior to the addition of iron and ascorbate. Protection against *Bam*HI cleavage was also determined by incubating *Bam*HI with duplex DNA substrate containing one *Bam*HI recognition site, prepared from annealing oligonucleotide 1 with oligonucleotide 2 (shown below, *Bam*HI recognition site is underlined), before the addition of iron and ascorbate: oligonucleotide 1, 5′-CGC GGG CGG CGG ATC CGG GCG GC-3′; oligonucleotide 2, 3′-GCG CCC GCC GCC TAG GCC CGC CG-5′.

The oligonucleotides were prepared in ddH_2O. The final concentration was 9.3 μM as determined from A_{260} measurements.

Sodium Dodecyl Sulfate−Polyacrylamide Gel Electrophoresis. Precast 10 to 20% gradient SDS−polyacrylamide gels were purchased from either Owl Laboratories or Novex Laboratories. Electrophoresis was carried out at 35 mA at room temperature for approximately 3 h. The protein bands were visualized by staining with 0.1% Coomassie Brilliant Blue in 50% methanol and destained with 50% methanol and 10% acetic acid. To determine the amount of enzyme cleaved, the gels were scanned and the intensity of the bands

[1] Abbreviations: Caps, 3-(cyclohexylamino)-1-propanesulfonic acid; ddH_2O, distilled, deionized water; DTT, dithiothreitol; EDTA, ethylenediaminetetraacetic acid; MALDI-TOF, matrix-assisted laser desorption/ionization-time-of-flight mass spectroscopy; SDS−PAGE, sodium dodecyl sulfate−polyacrylamide gel electrophoresis; Tris, tris-(hydroxymethyl)aminoethane buffer, TBE, tris-(hydroxymethyl)aminoethane borate ethylenediaminetetraacetic acid buffer; UV, ultraviolet.

was analyzed by NIH Image software. The cleavage rates for *Bam*HI were determined from the linear portion of the plots generated using the computer program MSExcel97. Molecular mass markers were used to estimate the mass of the Fe^{2+}/ascorbate-generated protein cleavage fragments that had been run on SDS−polyacrylamide gels.

Isolation of Protein Fragments and Protein Sequencing. Protein samples were run on 10 to 20% gradient Novex SDS−polyacrylamide gels. The gels were electroblotted on to Pro-Blott membranes [poly(vinylidene difluoride)]. The electroblotting was conducted in a blotting cassette (Bio-Rad) at a constant 150 mA current for approximately 12 h at 4 °C in 0.01 M Caps buffer, pH 11. Successful transfers were estimated at greater than 95% protein transfer from the gel to the membrane. After transfer, the protein bands were visualized by staining with 0.1% Coomassie Brilliant Blue in 50% methanol and destained with 50% methanol and 10% acetic acid. The membranes containing the transblotted protein fragments were stored at −80 °C until sequencing could be performed.

Automated sequence analyses were performed with a gas-phase Applied Biosystems protein sequencer (model 470A). Transblot membranes containing 3−6 nmol of protein fragments were directly sequenced by N-terminal Edman degradation. When insufficient samples of individual protein fragments were recovered from electroblotting, the digested protein was sequenced as a mixture without fragment purification.

RESULTS

Fe^{2+}/Ascorbate Inactivation of BamHI Nuclease Activity. The addition of 40 μM $FeSO_4$ in the presence of 10 mM ascorbate to 2 μM *Bam*HI at 25 °C causes a rapid and irreversible inactivation of *Bam*HI within 10 min as determined by DNA cleavage assays. Replacing ferrous sulfate with magnesium sulfate or removing ferrous sulfate or ascorbate from the reaction mix did not lead to inactivation. An apparent first-order inactivation rate constant of 0.3 ± 0.1 min^{-1} was obtained from the slope of the line as determined from the plots of log % activity vs time (data not shown).

Inactivation was also examined under anaerobic conditions. Argon gas was bubbled through a solution containing 100 mM KCl, 10 mM Bis-Tris-propane (pH 7.4), and 0.2 μg of BSA for 60 min to displace O_2 from the solution. *Bam*HI (2 μM) was then added to 1 mL aliquots of this buffer. While continuing to purge with argon gas, Fe^{2+} and ascorbate were added to the enzyme solution. After mixing, the purging continued for an additional 30 min. At this time, an aliquot of the enzyme was assayed for activity. No loss of *Bam*HI activity was observed as compared to untreated controls (under aerobic conditions), suggesting that the endogenous oxygen found in solution is sufficient and required for inactivation under experimental conditions.

*Protection of BamHI against Fe^{2+}/Ascorbate-Induced Inactivation. Bam*HI was treated with Fe^{2+} and ascorbate in the presence and absence of 4 mM Mg^{2+} and then assayed for its ability to cleave DNA. Mg^{2+} affords full protection against *Bam*HI inactivation from treatment with Fe^{2+} and ascorbate (data not shown), suggesting that the inactivation process specifically occurs at the Mg^{2+}-binding site on

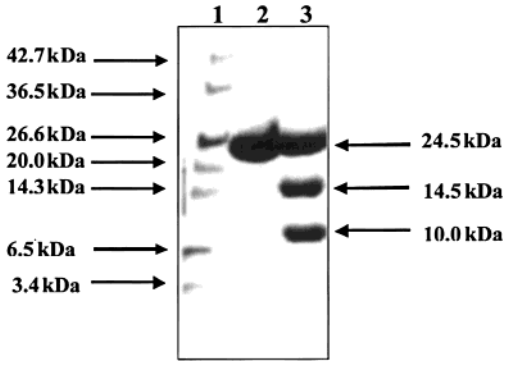

FIGURE 1: SDS−PAGE (10−20%) of Fe^{2+}/ascorbate-inactivated *Bam*HI. Lane 1, molecular mass markers; lane 2, *Bam*HI (untreated control); lane 3, *Bam*HI (2 μM) following treatment with Fe^{2+}/ascorbate.

*Bam*HI. Lower concentrations of Mg^{2+} also provided substantial, but reduced, protection. An approximate K_I value of 1 mM for Mg^{2+} inhibition against *Bam*HI Fe^{2+}/ascorbate-induced inactivation was obtained, which is similar to the K_D for Mg^{2+} for *Bam*HI (unpublished observations).

Addition of 10 mM EDTA (pH 7.4) also afforded 100% protection. The addition of 10 mM EDTA to a partially modified enzyme stopped further inactivation, providing the opportunity to quench the reaction at various time intervals and allowing for the exploration of time dependent inactivation and protein cleavage rates.

*Site-Specific Protein Cleavage of BamHI. Bam*HI inactivated by Fe^{2+}/ascorbate was subjected to SDS−PAGE to examine the possible oxidative cleavage of the polypeptide chain. Monomeric *Bam*HI has a M_r of 24.5 kDa. As seen in Figure 1, lane 3, the Fe^{2+}/ascorbate-inactivated enzyme clearly shows the presence of three bands, one at 24.5 kDa indicating uncleaved protein and two new bands at 14.5 and 10.0 kDa. This suggests that *Bam*HI was partially but specifically cleaved at a single site. Replacing Fe^{2+} with Mg^{2+} or removing the ascorbate from the reaction mix did not lead to *Bam*HI cleavage, indicating that both Fe^{2+} and ascorbate were required for inactivation and cleavage. Scanning and quantitation of the gel indicate that 50% of the fully inactive *Bam*HI was cleaved.

Treatment of denatured (with 0.1% w/v SDS) *Bam*HI with Fe^{2+}/ascorbate results in no cleavage after 30 min as determined by SDS−PAGE (Figure 2, lane 10). Similarly, denaturing *Bam*HI by heat (5 min at 90 °C) followed by treatment with Fe^{2+}/ascorbate also results in no cleavage after 30 min as determined by SDS−PAGE (Figure 2, lane 4). Intact native protein is required for the Fe^{2+}/ascorbate-induced inactivation and cleavage processes.

The time-dependent cleavage of *Bam*HI by Fe^{2+}/ascorbate was determined by quenching the reaction at various time intervals by the addition of 10 mM EDTA followed by SDS−PAGE separation. Figure 3 (inset) demonstrates that the addition of EDTA to an incubation mixture of the enzyme Fe^{2+} and ascorbate rapidly quenches the metal-catalyzed oxidative inactivation. A plot of % cleaved enzyme vs time is presented (Figure 3).

The apparent first-order rate constant for cleavage of 0.08 ± 0.01 min^{-1} was obtained from the slope of the line as determined from the plots of log % cleavage vs time. The apparent first order rate constant of cleavage is approximately

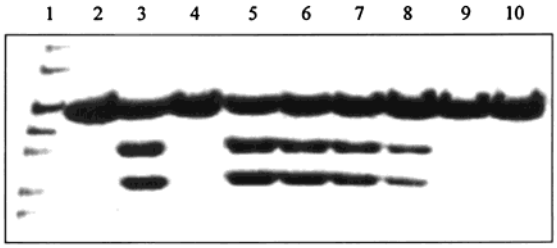

FIGURE 2: Effects of radical scavengers and denaturation on cleavage. In all cases except where indicated, *Bam*HI (2 μM) was incubated in the presence of Fe^{2+} (40 μM) and ascorbate (10 mM) for 30 min at pH 7.0. Lane 1 (molecular mass markers, from highest to lowest in kilodaltons), 42.7, 36.5, 26.6, 20.0, 14.3, 6.5, and 3.4; lane 2, untreated *Bam*HI (control); lane 3, *Bam*HI after treatment with Fe^{2+}/ascorbate; lane 4, *Bam*HI denatured by heat followed by treatment with Fe^{2+}/ascorbate; lane 5−9, incubated with glycerol followed by treatment with Fe^{2+}/ascorbate; lane 5, 0.01 mM glycerol; lane 6, 0.1 mM glycerol; lane 7, 1 mM glycerol; lane 8, 10 mM glycerol; lane 9, 50 mM glycerol; lane 10, *Bam*HI denatured by SDS followed by treatment with Fe^{2+}/ascorbate.

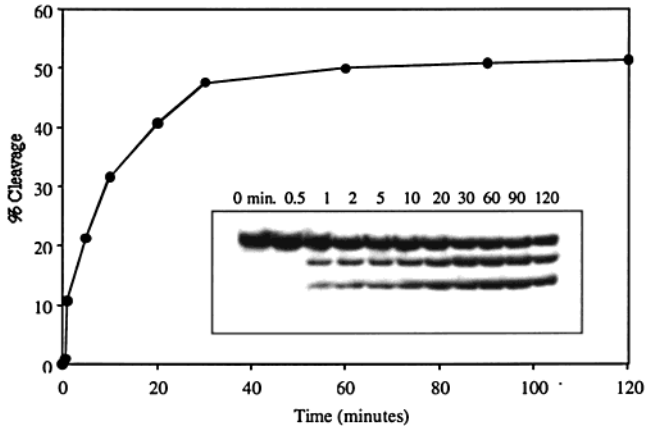

FIGURE 3: Rate of protein cleavage. *Bam*HI (2 μM) was incubated in the presence of 40 μM Fe^{2+} and 10 mM ascorbate. EDTA (10 mM) was added to the samples at the times indicated and the samples were then subjected to electrophoresis. The gel, which appears as an inset in the figure, was scanned and quantitated using NIH Image software. The reaction times are noted above the gel.

four times slower than the apparent first-order rate constant for enzyme inactivation under identical conditions.

Protection of BamHI against Fe^{2+}/Ascorbate-Induced Protein Cleavage. *Bam*HI (2 μM) was incubated with 3.1 μM oligonucleotide containing a single *Bam*HI recognition site, 400 μM Fe^{2+}, and 10 mM ascorbate. Excess iron was added to account for potential DNA−Fe^{2+} interactions. This mixture was equilibrated to pH 7.0 and the reaction proceeded for 30 min at room temperature. As shown in Figure 4*A*, lane 7, oligonucleotide substrate fully protects *Bam*HI from Fe^{2+}/ascorbate-induced cleavage suggesting that the protein cleavage reaction occurs at the *Bam*HI active site.

Mg^{2+}, Mn^{2+}, Co^{2+}, Ca^{2+}, and Cu^{2+} were examined for their effect on Fe^{2+}/ascorbate-induced protein cleavage of *Bam*HI. Figure 4A shows that all of the above divalent cations, except Cu^{2+} (Figure 4A, lane 3), fully protect *Bam*HI from Fe^{2+}/ascorbate-induced protein cleavage. The effect of Mg^{2+} concentration (Figure 4B) on protein cleavage was also examined. As Mg^{2+} concentration increased, enhanced protection against cleavage was observed. At 4 mM Mg^{2+} (100 M excess over Fe^{2+}; lane 4 in Figure 4B), complete protection against Fe^{2+}/ascorbate-induced cleavage was

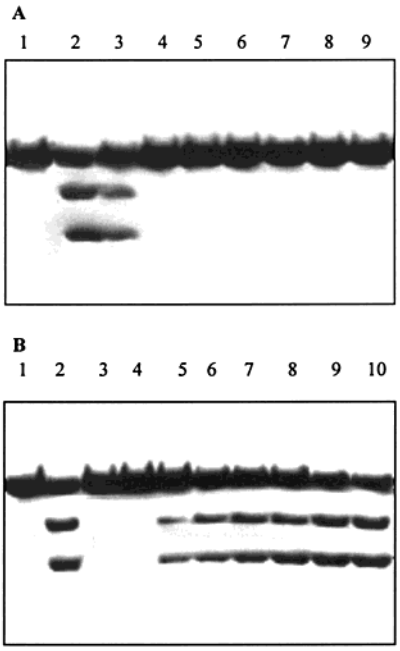

FIGURE 4: Ligand protection studies against Fe^{2+}/ascorbate protein cleavage. Additional ligands were added as indicated. After 30 min incubation, the reactions were quenched by the addition of 10 mM EDTA and the samples were subjected to SDS−PAGE. (A) Lane 1, *Bam*HI (2 μM) untreated; lane 2, *Bam*HI incubated in the presence of 40 μM Fe^{2+} and 10 mM ascorbate for 30 min at pH 7; Lane 3, as in lane 2 with 4 mM Cu^{2+}; lane 4, as in lane 2 with 4 mM Mg^{2+}; lane 5, as in lane 2 with 4 mM Mn^{2+}; lane 6, as in lane 2 with 4 mM Co^{2+}; lane 7, as in lane 2 with 4 mM Ca^{2+}; lane 8, as in lane 2 but with 400 μM Fe^{2+} and with 3.1 μM oligonucleotide substrate containing a single *Bam*HI recognition site; lane 9, as in lane 1; (B) lane 1, *Bam*HI (2 μM) untreated; lane 2, *Bam*HI incubated in the presence of 40 μM Fe^{2+}; lane 3, as in lane 2 with 10 mM Mg^{2+}; lane 4, as in lane 2 with 4 mM Mg^{2+}; lane 5, as in lane 2 with 1 mM Mg^{2+}; lane 6, as in lane 2 with 0.5 mM Mg^{2+}; lane 7, as in lane 2 with 0.1 mM Mg^{2+}; lane 8, as in lane 2 with 0.05 mM Mg^{2+}; lane 9, as in lane 2 with 0.01 mM Mg^{2+}; lane 10, as in lane 2.

observed. Half-maximal protection is observed at 1 mM Mg^{2+}. This value agrees with the K_D value for Mg^{2+} for *Bam*HI (unpublished observations) and is similar to the K_I for Mg^{2+} inhibition of Fe^{2+}/ascorbate-induced *Bam*HI inactivation (see above).

Radical Scavenger Effect on BamHI Cleavage. The effect of the addition of the radical scavenger glycerol to the Fe^{2+}/ascorbate-induced cleavage of *Bam*HI was examined. As shown in Figure 2, lanes 5−9, increasing concentrations of glycerol afforded increasing protection from cleavage. While 50 mM glycerol does not effect *Bam*HI DNA cleavage activity, total protection against Fe^{2+}/ascorbate-induced protein cleavage and inactivation (activity data not shown) was observed at 50 mM glycerol. These results suggest that the inactivation and subsequent cleavage processes may be due to radical reactions at the metal-binding site of *Bam*HI.

Sequence Analysis of the BamHI Cleavage Products. Fe^{2+}/ascorbate-digested *Bam*HI was subjected to N-terminal Edman degradation sequence analyses. A total of 17 cycles was run, with peaks corresponding to two amino acids in each of the first 15 cycles. As shown in Table 1, two series of amino acid sequences can be arranged to align with the known sequence of *Bam*HI. Sequence 1 corresponds to amino acids 1−17 of *Bam*HI, which constitutes both uncleaved *Bam*HI and the 10 kDa N-terminal *Bam*HI fragment.

Table 1: Amino Acid Sequences of Peptides from the Fe^{2+}/Ascorbate Digest of *Bam*HI

	cycle no.																
	1	2	3	4	5	6	7	8	9	10	11	12	13	14	15	16	17
*Bam*HI (1−17)	M	E	V	E	K	E	P	I	T	D	E	A	K	E	L	L	S
sequence 1	M	E	V	E	K	E	P	I	T	D	E	A	K	E	L	L	S
*Bam*HI (78−92)	K	P	L	D	I	L	K	L	E	K	K	K	G	G	P		
sequence 2	K	P	L	D	I	L	K	L	E	K	K	K	G	G	P		

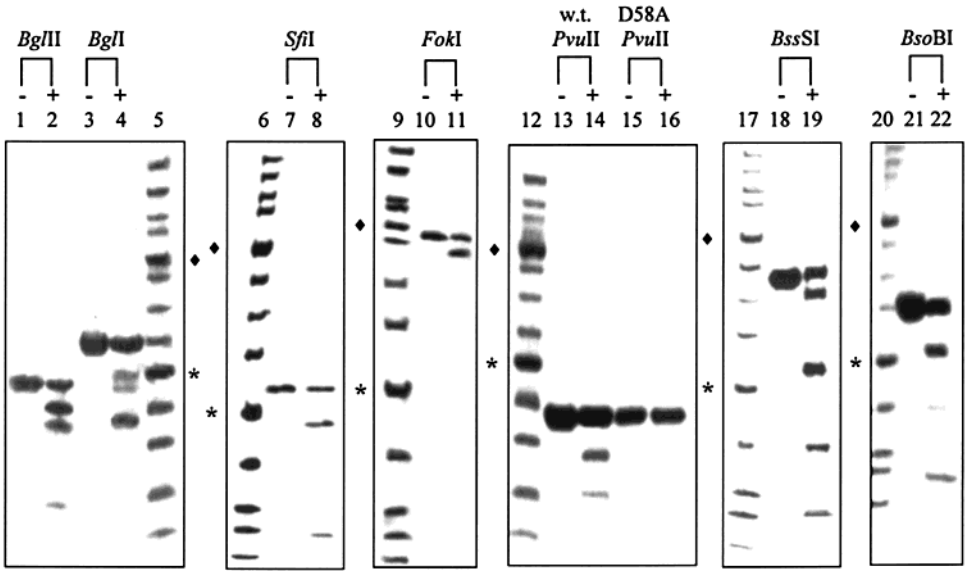

FIGURE 5: SDS (10−20%) of Fe^{2+}/ascorbate-treated endonucleases. The endonucleases are indicated above each lane. (−) Untreated enzyme. (+) Enzyme treated with 20 μM Fe^{2+} and 10 mM ascorbate at room temperature and at pH 7 for the indicated time. Lane 1, *Bgl*II (−); lane 2, *Bgl*II (+) 30 min; lane 3, *Bgl*I (−); lane 4, *Bgl*I (+) 24 h; lane 5, molecular mass markers (MMM); lane 6, MMM; lane 7, *Sfi*I (−); lane 8, *Sfi*I (+) 24 h; lane 9, MMM; lane 10, *Fok*I (−); lane 11, *Fok*I (+) 24 h; lane 12, MMM; lane 13, *Pvu*II (−); lane 14, *Pvu*II (+) 30 min; lane 15, Asp58Ala mutant of *Pvu*II (−); lane 16, Asp58Ala mutant of *Pvu*II (+) 24 h; lane 17, MMM; lane 18, *Bss*SI (−); lane 19, *Bss*SI (+) 24 h; lane 20, MMM; lane 21, *Bso*BI; lane 22, *Bso*BI (+) 6 h. The MMM, in kDa, are (from highest to lowest) 212; 158; 116; 97; 66.4 (◆); 55.5; 42.7; 36.5; 26.6 (*); 20.0; 14.3; 6.5; and 3.4.

Sequence 2 corresponds to amino acids 78−92 of *Bam*HI, which is the 14.5 kDa C-terminal *Bam*HI protein fragment. This result indicates that the site of cleavage is between Glu77 and Lys78, suggesting that Glu77 is involved in metal ligation. This is consistent with the three-dimensional structure for *Bam*HI, which identifies Glu77 as a ligand to the divalent cation (*1*, *2*).

Fe^{2+}/Ascorbate-Induced Protein Cleavage of Other Type II and Type IIs Endonucleases. The endonucleases *Pvu*II, *Fok*I, *Bgl*I, *Eco*RI, and *Eco*RV, all of which have known three-dimensional structures, as well as *Bgl*II, *Sfi*I, *Bss*SI, *Bso*BI, *Hin*P1I, and *Msp*I were incubated with Fe^{2+}/ascorbate.

Each enzyme was dialyzed, treated with Chelex-100, and separately incubated with Fe^{2+}/ascorbate (as described under Materials and Methods). At selected time intervals, 10 mM EDTA was added to each protein solution. The protein mixtures were then subjected to activity measurements and SDS−PAGE. Specific reaction conditions for each protein are provided in the legend for Figure 5.

The SDS−PAGE cleavage patterns of the Fe^{2+}/ascorbate-treated endonucleases are presented in Figure 5. *Bgl*I, *Bgl*II, *Sfi*I, *Fok*I, *Pvu*II, *Bss*SI, and *Bso*BI all showed substantial protein cleavage (approximately 50%) following treatment with Fe^{2+}/ascorbate at pH 7. Each enzyme was inactivated upon incubation with Fe^{2+}/ascorbate after 30 min. No DNA-nicking events were observed by the Fe^{2+}/ascorbate-treated enzymes. Minimal protein cleavage for each enzyme was always observed after 30 min; however, maximal cleavage for some endonucleases was observed at 24 h (reaction times are noted in the figure legend). No further digestion of any protein was observed after 24 h. Replacing Fe^{2+} with Mg^{2+} or removing the ascorbate from the reaction mix did not lead to inactivation or cleavage of any protein. Approximately 50% of each protein remained after maximal cleavage (Figure 5).

The effect of Mg^{2+} on Fe^{2+}/ascorbate-induced protein cleavage for *Bgl*I, *Bgl*II, *Sfi*I, *Fok*I, *Pvu*II, *Bss*SI, and *Bso*BI was examined. At 4 mM Mg^{2+} (200 molar excess over Fe^{2+}), complete protection against Fe^{2+}/ascorbate-induced cleavage was observed for all proteins (data not shown). The metal inhibition of Fe^{2+}/ascorbate-induced protein cleavage suggests that cleavage specifically occurs at or near the divalent metal-binding site for all of these proteins.

*Sfi*I, *Fok*I, and *Pvu*II (Figure 5, lanes 8, 11, and 14, respectively) showed the formation of two Fe^{2+}/ascorbate-induced protein cleavage products, suggesting that each enzyme was partially but specifically cleaved at a single site. A second faint cleavage product was observed at approximately 10 kDa for *Fok*I (not visible in Figure 5). *Bgl*II, *Bgl*I, *Bss*SI, and *Bso*BI (Figure 5, lanes 2, 4, 19, and 22, respectively) produced more than two cleavage products, indicating multiple sites of cleavage. In each case, there were a primary (darker bands) and secondary (fainter bands) set

Table 2: Summary of Fe^{2+}-Mediated Oxidative Cleavage Results on Various Endonucleases

enzyme	monomeric M_r (kDa)	cleavage fragments (kDa)[a]	cleavage site[b]	catalytic residues[c]
*Bam*HI	24.6	14.6 and 10.0	E77↓K78	E77, D94, E111, and E113 (*1*, *2*)
FokI	66.2	56 and 10.2	D450↓G451	D450, D467, and K469 (*3*)
*Bgl*I	34.0	20 and 14	D142↓I143	E87, D116, D142, and K144 (*7*)
*Pvu*II	18.3	12 and 6.3	D58↓A59	E55, D58, E68, and K70 (*8*)
*Bso*BI	36.7	26.7 and 10	D246↓P247	D124, D212, D246, and E252 (*20*)
*Bgl*II	25.8	21 and 4.8	D49↓P50	
*Sfi*I	31.0	26.0 and 5.0	D198↓P199	
*Bss*SI	51.8	31 and 20.8	A270↓K271	
*Eco*RI	30.9	nonspecific		D59, D91, E111, and K113 (*5*)
*Eco*RV	28.5	nonspecific		E45, D74, D90, and K92 (*6*)
*Msp*I	29.8	nonspecific		
*Hin*P1I	28.8	nonspecific		

[a] Fe^{2+}/ascorbate-induced cleavage of the various endonucleases was observed by SDS−PAGE as described within the text. [b] As determined from N-terminal sequence analyses of the cleavage fragments. [c] As identified by the three-dimensional structures or from mutational studies for each of these enzymes (see reference).

of cleavage products. On the basis of the fact that more than one amino acid is involved in metal binding (*1*−*8*), cleavage at more than one site is not unexpected.

Table 2 summarizes the Fe^{2+}-mediated oxidative cleavage N-terminal sequencing results for *Pvu*II, *Fok*I, *Bgl*I, *Bgl*II, *Sfi*I, *Bso*BI, and *Bss*SI. Sequence analyses revealed that cleavage occurred immediately after Asp58 for *Pvu*II, Asp450 for *Fok*I, and Asp142 for *Bgl*I (Table 2). These aspartic acid residues have also been identified as playing a role in metal ligation based on their corresponding three-dimensional structures (*3*, *7*, *8*). Two sequences appeared in the 10 kDa fragment for *Bso*BI. One sequence corresponded to the cleavage site at Asp246. Asp246 in *Bso*BI was identified by mutational studies as a critical amino acid residue (*20*). The second sequence in the 10 kDa fragment matched the N-terminus of *Bso*BI, suggesting that a secondary site of cleavage occurs approximately 10 kDa from the N-terminus in *Bso*BI.

The N-terminal sequencing results of the oxidative cleavage of *Bgl*II, *Sfi*I, and *Bss*SI (Table 2) suggest that Asp49 for *Bgl*II, Asp198 for *Sfi*I, and Lys271 for *Bss*SI are involved in metal ligation. Because of the unexpected nature of the *Bss*SI cleavage site (between an Ala/Lys), the *Bss*SI cleavage site was also confirmed via MALDI-TOF analysis (data not shown). An additional site of cleavage at Asp84 may also occur for *Bgl*II based on size of the Fe^{2+}/ascorbated-induced cleavage products for *Bgl*II. Amino acid sequence analyses of secondary cleavage products for *Bgl*I, *Bgl*II, *Bss*SI, and *Bso*BI were not possible as the fragments appeared to be N-terminally blocked.

Several enzymes, *Eco*RI, *Eco*RV, *Hin*P1I, and *Msp*I, did not generate specific fragments upon treatment with Fe^{2+}/ascorbate (Table 2), although all were inactivated. Figure 6 shows the SDS−PAGE cleavage patterns for Fe^{2+}/ascorbate-treated *Eco*RI and *Eco*RV. Both Fe^{2+}/ascorbate-treated enzymes did not produce specific cleavage fragments (Figure 6, lanes 3 and 5) using 20 μM Fe^{2+} and 10 mM ascorbate, pH 7.0 for 30 min (the conditions where specific cleavage was observed for *Bam*HI, *Pvu*II, *Bgl*I, *Bgl*II, *Bso*BI, *Sfi*I, and *Bss*SI) compared to the untreated controls. Rather, a "smear" pattern was produced. Similar "smear" patterns on the SDS−PAGE were also produced for *Hin*P1I and *Msp*I (data not shown). Numerous experimental conditions were examined, including a range of iron concentrations (20 μM to 1 mM),

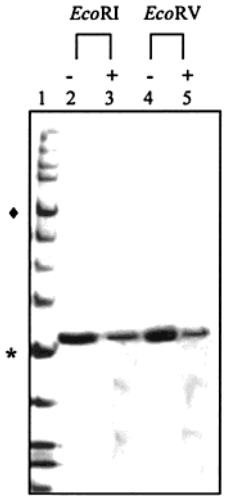

FIGURE 6: SDS−PAGE (10−20%) of Fe^{2+}/ascorbate-treated *Eco*RI and *Eco*RV. The endonucleases are indicated above each lane. (−) Untreated enzyme. (+) Enzyme-treated with 20 μM Fe^{2+} and 10 mM ascorbate at room temperature and at pH 7 for the indicated time. Lane 1, *Eco*RI (−); lane 2, *Eco*RI (+) 24 h; lane 3, *Eco*RV (−); lane 4, *Eco*RV (+) 24 h; lane 5, molecular mass markers. Fe^{2+}/ascorbate digestion of each enzyme resulted in over 50% nonspecific cleavage of the starting material for each enzyme. The molecular mass markers are the same as those used in Figure 5. (◆) 66.4 kDa band; (*) 26.6 kDa band.

a range of ascorbate concentrations (4−20 mM), a variety of pHs (3−7), a range of incubations times (30 min to 48 h), the addition of H_2O_2 (10 mM), and the removal of KCl from the dialysis solution (to limit the salt-enzyme interactions). No discrete cleavage products were formed for *Eco*RI, *Eco*RV, *Hin*P1I, and *Msp*I under any experimental conditions used. As was observed with *Bam*HI, approximately 50% of *Eco*RI, *Eco*RV, *Hin*P1I, and *Msp*I was cleaved following treatment with Fe^{2+} and ascorbate; however, the cleavage occurred at nonspecific sites (see Figure 6). Under the conditions employed, Fe^{2+} may not have associated tightly at the metal-binding sites of *Eco*RI, *Eco*RV, *Hin*P1I, and *Msp*I, thus accounting for nonspecific cleavage. It should be noted that all proteins, even those that exhibited specific cleavage under "normal" conditions (20 μM Fe^{2+} and 10 mM ascorbate, pH 7.0 for 30 min), showed nonspecific cleavage under "extreme" conditions (1 mM Fe^{2+} and 20 mM ascorbate, at pH 3 for 24 h). It is believed that this

nonspecific cleavage may be due to protein surface cleavage events caused by acid hydrolysis.

Fe^{2+}/Ascorbate Treatment of Asp58Ala Mutant of PvuII. *Pvu*II was inactivated and specifically cleaved (see Figure 5, lanes 13 and 14) when incubated with ferrous sulfate and ascorbate. Asp58 was identified as the site of cleavage generated from the Fe^{2+}/ascorbate treatment of *Pvu*II (Table 2). Mutating Asp58 of *Pvu*II to an alanine inactivates the protein (*23*). The Asp58Ala mutant of *Pvu*II was subjected to Fe^{2+}/ascorbate treatment. Figure 5, lanes 13−16, shows the SDS−PAGE pattern of wild-type *Pvu*II, wild-type *Pvu*II following treatment with Fe^{2+} and ascorbate (30 min), *Pvu*II with the Asp58Ala mutation, and the *Pvu*II with the Asp58Ala mutation following treatment with Fe^{2+} and ascorbate (24 h), respectively. Distinct cleavage products are observed for wild-type *Pvu*II as discussed above. However, even after 24 h, no specific cleavage products were observed for the Asp58Ala mutant of *Pvu*II. This result is consistent with the observation that Asp58 of *Pvu*II is involved in coordination of the divalent metal (*23*).

DISCUSSION

The three-dimensional structures of *Bam*HI, *Eco*RI, *Eco*RV, *Fok*I, *Pvu*II, *Bgl*I, and *Cfr*I0I are known (*1*−*8*). While these Type II restriction endonuclease structures are somewhat superimposable, there is little amino acid sequence similarity. Attempts to create sequence alignments of Type II restriction endonucleases have been met with limited success. One of the common features of these enzymes is that two or more carboxyl moieties, from either Asp or Glu, are involved in the coordination of divalent cations, and when examined in structural space, these catalytic residues are superimposable (*2*, *5*−*7*). To make further progress on identifying similar structural elements within this group of proteins, it may be helpful to find anchor points to begin aligning the sequences. This paper proposes a relatively rapid and simple method, using Fenton chemistry techniques (*9*), to identify critical residues to help align proteins of similar three-dimensional structures but with little obvious sequence similarity.

The work presented here demonstrates the validity of using Fenton chemistry techniques (*9*) to determine which residues in restriction endonucleases are involved in divalent metal ligation. In particular, the effect of Fe^{2+} oxidation on *Bam*HI endonuclease was examined. The atomic radius of Fe^{2+} is within 0.1 Å of that for Mg^{2+} and Mn^{2+}; therefore, it is possible that Fe^{2+} could occupy the divalent binding sites of proteins. *Bam*HI has an absolute requirement for divalent cations for activity, and the three-dimensional structure of *Bam*HI in the presence of DNA has revealed that Glu77, Asp94, and Glu111 provide ligands to the enzyme-bound metal (*1*, *2*). The results presented here indicate that *Bam*HI was inactivated and specifically cleaved with Fe^{2+}/ascorbate (Fenton chemistry) within 10 min. Approximately 50% of the enzyme is cleaved. The presence of undigested enzyme suggests that other oxidation processes besides cleavage must account for enzyme inactivation. It is possible that the native protein is susceptible to one cleavage reaction per dimer. Once one monomer is cleaved, the enzyme is inactive. An alternative possibility that must be considered is that only 50% of the starting enzyme was active. This would account for the complete loss in activity but only partial protein cleavage.

No further cleavage was observed with incubation times greater than 24 h (data not shown). The specific cleavage generates a 10 and a 14.5 kDa fragment. Denatured *Bam*HI (either by heat or SDS) is not cleaved. This indicates that the enzyme must be intact (full tertiary structure) in order for cleavage to occur. Protection from cleavage is observed by Mg^{2+}, Mn^{2+}, Co^{2+}, and Ca^{2+}. Mg^{2+} also protects against *Bam*HI Fe^{2+}/ascorbate-induced inactivation. The metal inhibition of Fe^{2+}/ascorbate-induced *Bam*HI cleavage suggests that protein cleavage occurs at the divalent metal-binding site. This result also demonstrates that metal binds to *Bam*HI in the absence of DNA.

DNA also fully protects *Bam*HI from Fe^{2+}/ascorbate-induced cleavage (Figure 4*A*, lane 7). This result contrasts those found with *Taq*I endonuclease where additional cleavage products were generated when *Taq*I was incubated with Fe^{2+}, ascorbate, and 5 μM oligonucleotide substrate containing a single *Taq*I recognition site (*19*). DNA may prevent access of ascorbate and/or oxygen to the metal site on the enzyme accounting for the observed protection against protein cleavage.

When Fe^{2+}/ascorbate-inactivated *Bam*HI was subjected to SDS−PAGE, only one cleavage site was detected. N-Terminal sequence analysis identified this cleavage site as being between Glu77 and Lys78. These results are consistent with the role that Glu77 is known to play in metal ligation as determined by three-dimensional structure studies and genetic analysis (*1*−*2*, *21*). Asp94 and Glu111 are also known to play a role in metal ligation (*1*, *2*), although no cleavage was observed near these amino acids. One possible reason for the lack of cleavage at these residues may be that Glu77 plays a larger role in metal ligation in the absence of DNA. The three-dimensional structure for *Bam*HI was resolved in the presence of DNA, whereas this work was done in the absence of DNA (since DNA afforded full protection against cleavage). Viadiu and Aggarwal (*2*) have shown that, in the absence of DNA, Glu77 plays a significant role in metal binding in the early part of the *Bam*HI catalytic reaction. As the reaction proceeds, there is an apparent "shift" of the metal site toward Asp94 and Glu111. In the presence of DNA, Asp94 and Glu111 appear to play a larger role in metal binding. The identification of only one critical amino acid residue using Fenton chemistry techniques is not unique to *Bam*HI. Similar results were found for *Fok*I, *Bgl*I, and *Pvu*II (Table 2).

*Fok*I, *Bgl*I, *Bgl*II, *Pvu*II, *Sfi*I, *Bss*SI, and *Bso*BI were fully inactivated following treatment with Fe^{2+}/ascorbate, but approximately only 50% of each enzyme was specifically cleaved (Figure 5). The fact that only 50% of these enzymes were cleaved further suggests that other oxidative events occur at the active sites for these enzymes that causes inactivation but does not lead to protein cleavage.

Partial Fe^{2+}/ascorbate-induced protein cleavage is not unique to endonucleases. Upon incubation with Fe^{2+}/ascorbate, isocitrate dehydrogenase (*15*), malic enzyme (*16*), and phosphoenolpyruvate carboxykinase (*18*) were fully inactivated but only 50% cleaved. It is possible that, for homodimeric *Bam*HI, as soon as one monomer is inactivated or cleaved, the entire protein is inactive. This may then account for why *Bam*HI is fully inactivated but only 50% cleaved following treatment with Fe^{2+}/ascorbate. *Bam*HI may lose its tertiary and quaternary structures upon treatment with

Fe^{2+} and ascorbate. *Fok*I, *Bgl*I, *Bgl*II, *Pvu*II, *Sfi*I, *Bss*SI, and *Bso*BI may be analogous to *Bam*HI. That is, once one monomer is cleaved, the other monomer is not subjected to cleavage and the enzyme is inactive.

However, both malic enzyme and phosphoenolpyruvate carboxykinase are monomers and they too are fully inactivated but only 50% cleaved following treatment with Fe^{2+}/ascorbate. It appears that enzyme cleavage is only partially responsible for enzyme inactivation. There appear to be distinct steps in Fe^{2+}/ascorbate-induced protein inactivation and cleavage. After Fe^{2+} binds to *Bam*HI (or other enzymes), the Fe^{2+}/ascorbate system generates reactive oxygen species such as H_2O_2, OH, or O_2^- radicals (*9*). For *Bam*HI, these radicals react with the nearby metal ligand Glu77 as well as with other nearby susceptible amino acids to cause inactivation and subsequent cleavage of the polypeptide backbone. Hlavaty and Nowak (*18*) determined that cysteine and tryptophan residues may be modified upon treatment of protein with Fe^{2+}/ascorbate, which may account for why the apparent first-order rate constant for protein inactivation is faster than the apparent first-order rate constant for protein cleavage. After these alternative reactions occur, the metal-binding site may no longer be competent to bind metal, and therefore, complete cleavage of the metal site cannot occur.

The Fe^{2+}/ascorbate-induced cleavage of *Bam*HI is specific and generates two peptides, fragment I (sequence 1, Table 1), which corresponds to the N-terminal half of *Bam*HI (amino acids 1−77), and fragment II (sequence 2, Table 1), which corresponds to the C-terminal half of *Bam*HI (amino acids 78−213). The cleavage process could potentially render a modified N-terminus on fragment II that would prohibit Edman degradation amino acid sequencing. Since sequencing of this peptide was possible, this indicates that the new N-terminus of this peptide was not modified. The radical scavenger, glycerol, significantly inhibited cleavage of *Bam*HI. This indicates that polypeptide cleavage may be due to the formation of radicals at the metal-binding site. One proposed mechanism that utilizes a radical cleavage of the polypeptide backbone and allows for an unmodified N-terminus is presented by Platis et al. (*26*). This mechanism proposes that the cleavage of the polypeptide backbone is mediated by hydroxyl radical abstraction of the CH hydride and subsequent recombination with oxygen. The last step of this mechanism is the hydrolysis of the cyano group on the N-terminus of the C-terminal peptide. This process would generate a free N-terminus at the cleavage site allowing for Edman degradation amino acid sequencing. Edman degradation amino acid sequencing has also been performed on the peptides resulting from Fe^{2+}/ascorbate-induced cleavage of staphylococcal nuclease (*14*), isocitrate dehydrogenase (*15*), and malic enzyme (*16*), and phosphoenolpyruvate carboxykinase (*18*), indicating that a free N-terminus can be formed after oxidative cleavage of a polypeptide backbone. It should be noted that while the results presented here suggest a radical mechanism for cleavage, a hydrolytic mechanism for polypeptide backbone cleavage that would yield a free N-terminus is also possible (*27*). Other proposed mechanisms for cleavage of the polypeptide backbone may result in a modified N-terminus that would prohibit Edman degradation amino acid sequencing. Since several of the Fe^{2+}/ascorbate-generated cleavage products obtained from various proteins studied here could not be sequenced, it appears that distinct mechanisms for Fe^{2+}/ascorbate-induced protein cleavage occur at different sites.

The N-terminal sequence analyses of the cleavage fragments generated from the Fe^{2+}/ascorbate treatment of *Pvu*II, *Fok*I, *Bso*BI, and *Bgl*I identified in each an aspartic acid residue involved in metal ligation that agrees with their respective three-dimensional structures or mutational studies (*3*, *7*, *8*, *20*). Asp58 of *Pvu*II was identified by both its three-dimensional structure (*8*) and by this work as being a catalytic amino acid. When the Asp58Ala mutant of *Pvu*II was subjected to Fe^{2+}/ascorbate treatment, no protein cleavage was observed, further suggesting that Asp58 of *Pvu*II is involved in both metal ligation. These results, along with the *Bam*HI data, suggest that Fe^{2+}/ascorbate treatment of endonucleases is specific for the metal-binding sites on the enzymes.

Fenton chemistry techniques can be applied to endonucleases that do not have resolved three-dimensional structures in order to gain more information about their catalytic sites. This was done for the endonucleases *Bgl*II, *Sfi*I, and *Bss*SI (Figure 5, Table 2). The metal-binding sites of these enzymes are proposed (Table 2) based on the results obtained from Fe^{2+}-mediated oxidative cleavage of these enzymes. Asp198 and Lys271 are proposed as metal-binding residues for *Sfi*I and *Bss*SI, respectively. The cleavage site for *Bss*SI, between an Ala/Lys, was unexpected. The unusual arrangement of three acidic amino acids near Lys271 of *Bss*SI (Asp272, Glu273 and Asp274) may explain the observed cleavage. It may be possible that the pK_a for Lys271 was altered due to this highly charged environment. As such, Lys271 of *Bss*SI may be in an uncharged state and the lone electron pair on the nitrogen allows lysine to serve as a metal ligand. An alternative possibility is that one or more of the residues adjacent to Lys271 of *Bss*SI serve as ligands to the metal. Asp49 is proposed as a metal ligand for *Bgl*II. A secondary cleavage product of *Bgl*II (see Figure 5) indicates cleavage occurring at an additional site possibly at Asp84. Site-specific mutations are now being created at these residues for *Bgl*II and *Bss*SI to further investigate the role of those amino acids play in catalysis.

Several enzymes, *Eco*RI, *Eco*RV, *Hin*PI, and *Msp*I, did not generate specific fragments upon treatment with Fe^{2+}/ascorbate (Table 2, Figure 6). It is not known why these four endonucleases do not respond with a unique cleavage to Fenton chemistry, especially in view of the similarity of the structural aspects of some of these endonucleases. It is possible that either *Eco*RI, *Eco*RV, *Hin*PI, and *Msp*I have very low affinity for Fe^{2+} or Fe^{2+} binds nonspecifically to the surface of these proteins, thus resulting in the nonspecific protein cleavage.

A sequence alignment of the catalytic residues of the endonucleases studied in this work that have known three-dimensional structures or catalytic residues identified from mutational studies was created in Table 3. The general catalytic motif of PDX_{14-20}(E/D)*X*K, found in *Eco*RI and *Eco*RV (*5*, *6*), was used as a starting point for this alignment. On the basis of the three-dimensional structures *Eco*RI and *Eco*RV (*5*, *6*), this motif was proposed as the catalytic center and as the metal binding site for Type II endonucleases. While this site is also conserved in *Fok*I (*3*) and *Mun*I (*24*),

Table 3: Catalytic Residues for Various Endonucleases[a]

*Bam*HI [b]	E(77)↓K----------PID(94)V----------E(111)FE
*Fok*I [b]	PD(450)↓G----------D(467)TK
*Bgl*I [b]	E(87)K----------PD(116)E----------D(142)↓IK
*Pvu*II [b]	E(55)G-D(58)↓A--------E(68)LK
*Bso*BI [c]	D(212)I----------D(246)↓P---DE(252)H
*Eco*RI [b]	D(59)S----------PD(91)GG----------E(111)AK
*Eco*RV [b]	E(45)L----------PD(74)F----------D(90)IK

[a] Alignment of sequences based on mutational or three-dimensional structure data. The Fe^{2+}/ascorbate-induced cleavage site in each protein is indicated by the bold arrow (also see Table 2). Each dash represents one amino acid. No specific Fe^{2+}/ascorbate-induced cleavage site was identified for *Eco*RI and *Eco*RV (see text and Table 2). [b] Proteins with known three-dimensional structures. See Table 2 for references. [c] Catalytic residues determined from mutational studies (*20*).

immediate variations within this motif were found within the catalytic centers for *Bam*HI (*1*, *2*), *Pvu*II (*8*), and *Nae*I (*25*). The catalytic center of *Bam*HI has an isoluecine inserted into the PD doublet and the lysine is replaced by a glutamate in the (E/D)*X*K triplet (see Table 3). For both *Pvu*II and *Nae*I, no PD doublet is found upstream of the (E/D)*X*K triplet. As shown in Table 3, the Fe^{2+}/ascorbate-induced cleavage site varies significantly within this proposed catalytic motif (cleavage site is identified by the arrow) for these enzymes.

It appears that the catalytic residues for *Bgl*II, *Bso*BI, *Sfi*I, and *Bss*SI are distinct from the PDX_{14-20}(E/D)*X*K catalytic motif found in some other endonucleases. Cao and Barany (*19*) demonstrated that Fe^{2+}-mediated cleavage of *Taq*I endonuclease occurred at seven distinct positions. Asp137 and Lys157 were implicated as catalytic residues and are located adjacent to two of the cleavage sites. Cao and Barany also suggested that the critical amino acids for *Taq*I endonuclease are distinct from the PDX_{14-20}(E/D)*X*K catalytic motif. While earlier work (*1*, *2*, *5*, *6*, *8*) has suggested certain definable catalytic motifs, it is now becoming apparent that there are many exceptions that do not follow any definable motif. As more structures become available and as the precise roles that metals play in the endonuclease reactions become understood, other motifs may be proposed. Cleavage by Fenton chemistry may help elucidate different catalytic motifs in Type II endonucleases.

In summary, of the 12 restriction enzymes examined, five metal-binding sites have been confirmed and three new metal-binding residues have been identified. For *Bam*HI, it appears that the role the divalent metal plays in catalysis "shifts" as the reaction proceeds. While all 12 enzymes examined within this work share important catalytic features, their lack of homology at their respective active sites indicates the lack of any one dominant catalytic motif for Type II restriction enzymes. The catalytic centers of these proteins may vary far more than originally predicted. This work shows that Fenton chemistry techniques can be applied to identify the metal binding/catalytic residues of endonucleases and may be applicable for use in other endonuclease systems.

ACKNOWLEDGMENT

The authors wish to express their appreciation to Jurate Bitinaite, Rebecca Kucera, Marilena Hall, Paul Riggs, Robert Borsetti, Steve Picone, Chris Benoit, Lydia Dorner, and Shawn Stickel for supplying enzyme samples and for their valuable discussions. Thanks is extended to Geoffrey Wilson and Dan Heiter for their assistance with *Bss*SI and Paul Riggs for donating the Asp58Ala mutant of *Pvu*II. Special thanks is given to Don Comb and New England Biolabs for making this research possible.

REFERENCES

1. Newman, M., Strzelecka, T., Dorner, L. F., Schildkraut, I., and Aggarwal, A. K. (1995) *Science 269*, 656−663.
2. Viadiu, H., and Aggarwal, A. K. (1998) *Nat. Struct. Biol. 5*, 910−916
3. Wah, D., Hirsch, J. A., Dorner, L. F., Schildkraut, I., and Aggarwal, A. K. (1997) *Nature 388*, 97−100.
4. Bozic, D., Grazulis, S., Siksnys, V., and Huber, R. (1996) *J. Mol. Biol. 255*, 176−186.
5. Kim, Y., Grable, J. C., Love, R., Greene, P. J., Rosenberg, J. M. (1990) *Science 249*, 1307−1309.
6. Winkler, F. K., Banner, D. W., Oefner, D., Tsernoglou, D., Brown, R. S., Heatherman, S. P., Bryan, R. K., Martin, P. D., Petratos, K., and Wilson, K. S. (1993) *EMBO J. 12*, 1781−11795.
7. Newman, M., Lunen, K., Wilson, G., Greci, J., Schildkraut, I., and Phillips, S. E. V. (1998) *EMBO J. 17*, 5466−5476.
8. Cheng, X., Balendiran, K., Schildkraut, I., and Anderson, J. E. (1994) *EMBO J. 13*, 3297−3935.
9. Fenton, H. J. H. (1894) *J. Chem. Soc. 65*, 899−910.
10. Schepartz, A., and Cuenoud, B. (1990) *J. Am. Chem. Soc. 112*, 3247−3249.
11. Hoyer, D., Cho, J., and Schultz, P. G. (1990) *J. Am. Chem. Soc. 112*, 3249−3250.
12. Farber, J. M., and Levine, R. L. (1986) *J. Biol. Chem. 261*, 4574−4578.
13. Liaw, S.-H., Villafranca, J. J., and Eisenberg, D. (1993) *Biochemistry 32*, 7999−4003.
14. Ermácora, M. R., Delfino, J. M., Cuenoud, B., Schepartz, A., and Fox. R. O. (1992) *Proc. Natl. Acad. Sci. U.S.A. 89*, 6383−6387.
15. Soundar, S., and Colman, R. F. (1993) *J. Biol. Chem. 268*, 5264−5271.
16. Wei, C.-H., Wei-Yuan, C., Shih-Ming, H., Ching-Chun, L., and Gu-Gang, C. (1994) *Biochemistry 33*, 7931−7936.
17. Ettner, N., Metzger, J., Lederer, T., Hulmes, J. D., Kisker, C., Hinrichs, W., Ellestad, G. A., Hillen, W. (1995) *Biochemistry 34*, 22−31.
18. Hlavaty, J. J., and Nowak, T. (1997) *Biochemistry 36*, 15515−15525.
19. Cao, W., and Barany, F. (1998) *J. Biol. Chem. 273*, 33002−33010.
20. Ruan, H., Lunnen, K. D., Pelletier, J. J., Xu, S.-y. (1997) *Gene 188*, 35−39.
21. Xu, S.-y., and Schildkraut, I. (1991) *J. Biol. Chem. 266*, 4425−4429.
22. New England Biolab 1998/99 Catalog, pp 21−55.
23. Nastri, H. G., Evans, P. D., Walker, I. H., and Riggs, P. D. (1997) *J. Biol. Chem. 272*, 25671−25767.
24. Siksnys, V., Zareckaja, N., Vaisvila, R., Timinskas, A., Stakenas, P., Butkus, V., and Janulaitis, A. (1994) *Gene 142*, 1−8.
25. Holtz, J. K., and Topal, M. D. (1994) *J. Biol. Chem. 269*, 27286−27290.
26. Platis, I. E., Ermácora, M. R., and Fox, R. O. (1993) *Biochemistry 32*, 12761−12767.
27. Rana, T. M., and Meares, C. F. (1991) *Proc. Natl. Acad. Sci. U.S.A. 88*, 10578−10582.

BI992268C